Eurographics/ IEEE-VGTC Symposium on Visualization 2008
A. Vilanova, A. Telea, G. Scheuermann, and T. Möller
(Guest Editors)

Volume 27 (2008), Number 3

Physically-based Dye Advection for Flow Visualization

Guo-Shi Li[1], Xavier Tricoche[2], and Charles Hansen[1]

[1]Scientific Computing and Imaging Institute, School of Computing, University of Utah, USA
[2]Department of Computer Science, Purdue University, USA

Abstract

Dye advection is widely used in experimental flow analysis but has seen less use for visualization in computational fluid dynamics. One possible reason for this disconnect is the inaccuracy of the texture-based approach, which is prone to artifacts caused by numeric diffusion and mass fluctuation. In this paper, we introduce a novel 2D dye advection scheme for flow visualization based on the concept of control volume analysis typically used in computational fluid dynamics. The evolution of dye patterns in the flow field is achieved by advecting individual control volumes, which collectively cover the entire spatial domain. The local variation of dye material, represented as a piecewise quasi-parabolic function, is integrated within each control volume resulting in mass conserving transport without excessive numerical diffusion. Due to its physically based formulation, this approach is capable of conveying intricate flow structures not shown in the traditional dye advection schemes while avoiding visual artifacts.

Keywords: Flow Visualization, Dye Advection

1. Introduction

The advancements of computational fluid dynamics (CFD) [And95] research has resulted in a large number of flow datasets generated by numerical simulations. New technologies, such as particle imaging velocimetry (PIV) [SWK03], also offer new ways to obtain the quantitative measurements of flow fields from real-world experiments. One way to effectively inspect the numerical flow datasets of ever mounting size and complexity is to recreate the computational analogy of experimental techniques, since their visual interpretation has been well studied and understood in the experimental fluid analysis.

One such technique is dye advection, which imitates a scenario where the external dye material is continuously introduced into the flow field to depict global structures originating from the injection site. It has a long history in experimental fluid analysis and had contributed to many major discoveries. In the CFD community, however, the use of dye advection for the visual interpretation of the computational data is relatively limited. One possible explanation for this disconnect is the physical inconsistency between the visualization and the fluid simulation methodology. The standard approach of dye advection in the flow visualization community is based on the principle of semi-Lagrangian texture advection, e.g. [JEH00, Wei04]. In this method, intermediate Lagrangian points located at pixel centers are traced back in time to transport the dye material. Although this formulation is easy to understand and allows for efficient hardware accelerated implementations, it is inherently non-physical and has severe drawbacks. The first issue is numerical diffusion, which introduces artificial diffusive behavior into the resulting visualization. The second issue concerns the conservation of mass. It is known that the semi-Lagrangian advection scheme can spuriously increase or decrease the mass of dye material due to the lack of a *continuity formulation* [Rnc92]. As illustrated in figure 1, the combination of these two issues can result in misleading visualizations which in turn lead to an incorrect interpretation of the underlying flow physics. Although several correction schemes such as [JEH02, Wei04, SS04] have been proposed to tackle these issues, they remain non-physical and therefore introduce undesirable artifacts into the visualization.

To address these problems, in this paper we propose a physically-based dye advection scheme for flow visualiza-

© 2008 The Author(s)
Journal compilation © 2008 The Eurographics Association and Blackwell Publishing Ltd.
Published by Blackwell Publishing, 9600 Garsington Road, Oxford OX4 2DQ, UK and 350 Main Street, Malden, MA 02148, USA.

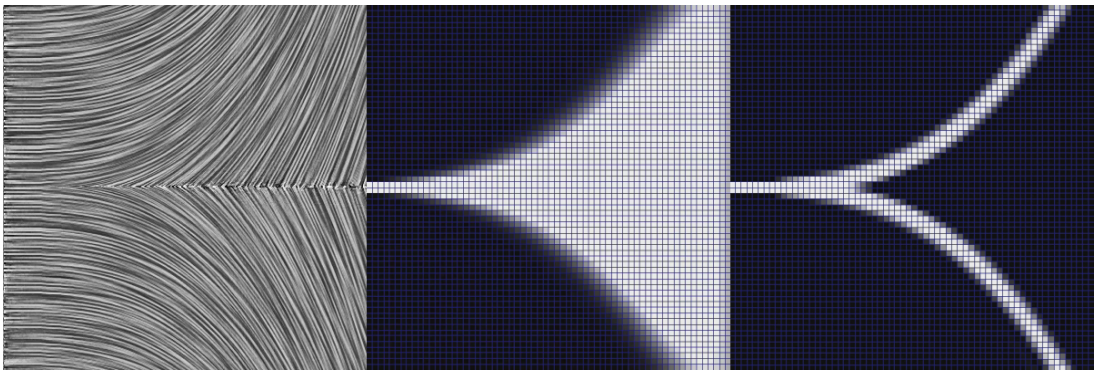

Figure 1: *Visualization of a synthetic flow exhibiting a splitting behavior. Left: dense texture visualization using GPU-FLIC [LTH06]. Middle: dye advection visualization by the semi-Lagrangian texture advection scheme. The pattern appears to be divergent and diffusive. Right: accurate visualization by the physically-based control volume dye advection scheme.*

tion based on the fluid dynamics concept of control volume. In this method, the transport of the dye material by the flow is achieved by advecting individual non-overlapping control volumes collectively representing the entire spatial domain. The local distribution of dye material within each control volume is represented as a piecewise quasi-parabolic function, which is integrated within control volumes to obtain the mass to be transported with less numerical diffusion [CW84]. The mass of the dye material is conserved during advection thanks to the physically-based construct. While not interactive, with this method the intricate structures in the numerical flow datasets can be faithfully conveyed without non-physical artifacts. Although similar concepts have been widely used in numerical simulations of various disciplines such as meteorology [BPL04] and astrophysics [SKFS05], to our knowledge it is yet to be utilized by the flow visualization community to achieve accurate dye advection visualization.

The rest of this paper is organized as follows. In Section 2 we review related work of dye advection for flow visualization. Section 3 discusses the background of material transport phenomenon using texture advection. The theoretical foundation of the physically based dye advection scheme based on control volume advection and integration is provided in Section 4, followed by implementation details in Section 5. The results, comparison to existing schemes, and discussion are provided in Section 6. Finally, we conclude the paper and point out possible future research avenues in Section 7.

2. Related Work

Introducing foreign material such as smoke and dye into the flow for visualization purposes has a long history in experimental fluid dynamics. Comprehensive discussions on this topic from the experimental aspects can be found in standard texts such as [Mer87]. In the flow visualization community, many methods had been proposed to create the computational analogy of experimental techniques. Max [MBC93] proposed the notion of the *flow volume* to visualize 3D flows, which iteratively creates a tetrahedral grid from a starting surface. The vertices of the starting surface are traced forward in time to form layers of prisms, which collectively constitute the spatial dispersion of dye material induced by the flow. It was later extended in [BML95] to unsteady flow. Since this approach only computes the outmost boundary of the dispersion phenomenon instead of the actual physical transport process, the resulting visualization cannot accurately convey the material distribution inside of the geometric grid.

Dye advection can also be implemented using the principle of texture advection. In this approach, the distribution of dye material is represented as a color texture which is evolved over time using the flow. Although methods belonging to this category are primarily designed for dense texture visualization, dye advection can be achieved when localized patterns instead of noise are advected in the texture. Shen et al. [SJM96] introduced a searching scheme to propagate the dye material in the texture space and combined it with LIC rendering [CL93] to highlight features in the flow field. Jobard et al. [JEH00] proposed to use the *dependent texture* functionality provided by the graphics hardware to iteratively advect and blend textures for flow visualization. Originally designed for steady flows, this method was later extended to handle unsteady flows and was referred to as *Lagrangian-Eulerian Advection* (LEA) [JEH01, JEH02]. Instead of per-pixel semi-Lagrangian backward advection in LEA, Image Based Flow Visualization by van Wijk [vW02] utilizes a coarser rectilinear grid to sample and warp the texture forward in time to achieve material transport. It is capable of emulating a wide range of dense texture flow visualization techniques as well as dye advection.

Texture advection methods are known to suffer from nu-

© 2008 The Author(s)
Journal compilation © 2008 The Eurographics Association and Blackwell Publishing Ltd.

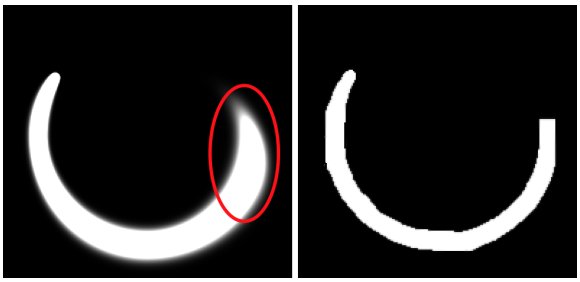

Figure 2: *Visual artifacts in non-physical texture advection. Left: numerical diffusion in the semi-Lagrangian texture advection scheme. Right: clamping-based correction schemes can cause unnaturally sharp patterns. If the correction is applied periodically, popping artifacts can occur due to patterns that alternatively exhibit blurring and sharp boundaries.*

merical diffusion. Jobard et al. [JEH02] introduced a clamping scheme to adjust the sharpness between the dye material and the background. Weiskopf [Wei04] modeled the interface between the dye material and the background as a level-set distance field which was periodically re-initialized to eliminate numerical dispersion. This scheme was later extended in [WBE05] to visualize flow divergence. Kim et al. [KLLR07] introduced an error compensation scheme into levelset computation to reduce diffusion and dispersion.

3. Transport of Dye Material with Texture Advection

There are several options to achieve the transport of dye material in the flow field. The purely Lagrangian approach, in which the dye released for advection is seen as a collection of individual particles, is impractical due to the prohibitively high computation and storage requirements. From the Eulerian standpoint, the conservation of dye material is described as a function of space and time and can be expressed as the following advection equation:

$$\frac{\partial \Phi}{\partial t} + v \cdot \frac{\partial \Phi}{\partial x} = 0 \tag{1}$$

where Φ and $\mathbf{v}$ are the material distribution function of the dye and the vector field, respectively. Since the direct solution to equation 1 has an *unconditionally unstable* error term with exponential growth [KK03], in the flow visualization community the texture advection scheme is therefore commonly used to avoid this problem. It is known as a semi-Lagrangian approach as the evolution of Φ is computed at each discrete pixel center $\mathbf{x}$ of the domain:

$$\Phi(\mathbf{x},t) = \Phi(\mathbf{x}',t-\Delta t) \tag{2}$$

where $\mathbf{x}'$ is the *departure point* leading to x and is computed by backward advection, and Δt denotes the size of the time step. Since $\mathbf{x}'$ in general does not coincide with grid points, interpolation is used to obtain $\Phi(\mathbf{x}',t-\Delta t)$. Although the semi-Lagrangian texture advection scheme is *unconditionally stable* even with relatively long time stepping [Sta99], it is subject to numerical diffusion due to the use of linear interpolation to sample Φ at $\mathbf{x}'$ [BFMF06]. Please see figure 2 (a). Because this smearing phenomenon results purely from the algorithm and is not related to the physical process, it can possibly lead to a wrong interpretation of the dataset under investigation. Although clamping based methods [JEH02, Wei04] have been proposed to suppress the numerical diffusion term, their practicality is limited due to their non-physical premise. The rate of the numerical diffusion introduced into the resulting visualization depends on many parameters, including the size of spatial and temporal discretization, and most importantly, the dynamics of the flow dataset itself. A single global threshold cannot properly deal with the aggregate influence of all these factors. As a result, in complicated flows it is difficult to distinguish whether a feature is introduced by small scale flow motion or numerical diffusion. This can cause the flow to appear frozen [JEH00], or lead to popping artifacts in which the patterns alternatively exhibit blurring and sharp boundaries if periodical resetting [Wei04] is employed. The resulting visualization also appears unnatural due to the binary dye/background interface. Please refer to figure 2 (b).

Another issue associated with this approach not yet addressed by the flow visualization community is the violation of the law of conservation. It is well recognized that the semi-Lagrangian scheme does not conserve invariant properties of the system, such as mass of humidity in meteorology [NM02] or vorticity in visual simulation of fluids [ETK*07]. This is because the interpolation polynomial can overshoot or undershoot within the fixed local stencil, causing artificial increase or decrease of mass to the system. As illustrated in figure 3, a slight difference in the flow field can cause either an increase or decrease of the total mass of the system with the same initial dye material distribution. In figure 1 (b), the dye pattern fails to branch due to the spurious increase of dye material, which in turn results in an erroneous visualization where the flow appears to be divergent. Although this problem can be partially mitigated with a monotonic interpolation function [FSJ01] or a posterior correction scheme [SS04], due to the lack of a continuity formulation these methods can only ensure global but not local mass conservation. Detailed discussion on this issue can be found in [Lau06].

4. Physically-based Dye Advection using Control Volume Transport

The issues discussed in the previous section can be overcome by a physically based formulation of the material transport phenomenon based on the concept of control volume analysis commonly used in fluid dynamics [And95]. A control

© 2008 The Author(s)
Journal compilation © 2008 The Eurographics Association and Blackwell Publishing Ltd.

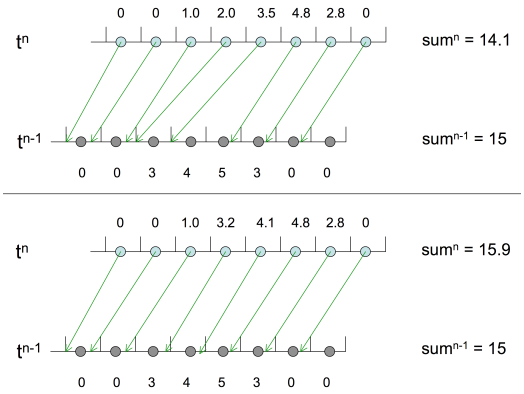

Figure 3: *1D illustration of the non-conservative nature of the semi-Lagrangian texture advection scheme. The total mass in the system can either decrease (top) or increase (bottom) depending on the behavior of the flow.*

volume is a closed system defined by virtual boundaries in the flow field. According to the Reynolds Transport Theorem [CC06], the total mass contained within a moving control volume traveling with the flow remains constant as the mass flux across its boundary is zero. The total mass to be transported to a given control volume V_i^n thus should be equal to that within V_i^{n-1}, the same control volume at a previous time. Using a figure of speech, it is equivalent to throwing a net upstream to "fetch" the total mass enclosed therein. Figure 4 provides a one-dimensional illustration of this process. To compute the evolution of dye patterns in the entire domain, it is discretized into non-overlapping control volumes which transport the mass individually. In this section, we discuss the foundation of this physically-based material transport scheme for dye advection.

4.1. Continuity Equation

Consider an one-dimensional control volume V_i with two arbitrary moving boundaries $x_1 = x_1(x,t)$ and $x_2 = x_2(x,t)$, integrating equation 1 then applying Leibnitz's rule [LP95] leads to:

$$\frac{d}{dt}\int_{x_1}^{x_2}\Phi dx - \left(\Phi(x_2)\frac{dx_2}{dt} - \Phi(x_1)\frac{dx_1}{dt}\right) + (\Phi(x_2)v(x_2) - \Phi(x_1)v(x_1)) = 0 \quad (3)$$

since the entire control volume is moving along the flow, i.e. $\frac{dx_1}{dt} = v(x_1)$ and $\frac{dx_2}{dt} = v(x_2)$, the above equation can be simplified to the following continuity form:

$$\frac{dM_{V_i}(x_1,x_2)}{dt} \equiv \frac{d}{dt}\left(\int_{x_1}^{x_2}\Phi(x)dx\right) = 0 \quad (4)$$

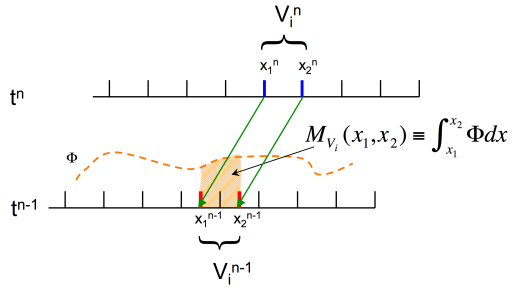

Figure 4: *Material transport via control volume integration. The total mass contained in V_i (shaded in orange) is computed by integrating Φ at t^{n-1}.*

which implies that total mass of the dye material M within control volume V_i remains invariant over time.

4.2. Control Volume Advection and Mass Integration

Based on the Reynolds Transport Theorem, the rate of change of the dye material within control volume V is:

$$\frac{d}{dt}\left(\int_{x_1^n}^{x_2^n}\Phi(x,t)dx\right) = \frac{d}{dt}\left(\int_{x_1^{n-1}}^{x_2^{n-1}}\Phi(x,t-\Delta t)dx + \int_{x_1^n}^{x_2^n}\mathcal{S}(x,t)dx\right) \quad (5)$$

where $\mathcal{S}$ represents the combined contribution of sink/source terms. Integrating both sides of equation 5 by time, the total mass of dye material transported to V at t can be obtained by integrating the material distribution function Φ within the interval defined by the boundary of V_i at $t-\Delta t$, plus the injection or removal of dye material made to V_i at t. In 1D the boundary of V_i at $t-\Delta t$, i.e. x_1^{n-1} and x_2^{n-1}, can be obtained by backward integration. In 2D, assuming the boundary of a control volume V_i^n is defined as a polygon, the same process is achieved by tracing its vertices back in time which are then connected together to form a new polygon denoting V_i^{n-1}. It can be shown that the boundary of a convex control volume traced back in time remains convex if the time stepping in terms of the Lipschitz number is not too large for the flow shear [SP92]. The complete evolution of Φ over time thus can be computed by evaluating equation 5 on every control volume, which collectively discretizes the entire spatial domain. The transport of dye material using this method is mass-conserving by construction.

4.3. Piecewise Quasi-parabolic Material Distribution

In addition to the physical foundation for conservative dye advection provided in section 4.1 to 4.2, the local variation of Φ in each control volume also needs to be specified to

© 2008 The Author(s)
Journal compilation © 2008 The Eurographics Association and Blackwell Publishing Ltd.

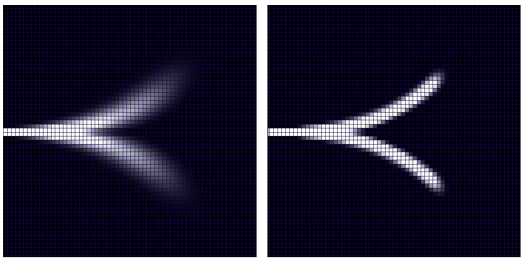

Figure 5: *Visualization results using (a) piecewise constant and (b) quasi-parabolic material distribution function.*

compute the integral in equation 5. Although mass conservation can be achieved with any parametric function satisfying equation 4, it can be shown that the naive choice, i.e., piecewise constant distribution, is mathematically equivalent to the first-order Euler-Forward scheme [LP95], which is excessively damped. In order to better capture the local variation of material distribution within each control volume, we opt for the piecewise quasi-parabolic representation by Nair and Machenhauer [NM02]:

$$\Phi_{i,j}(x,y) = \overline{\Phi_{i,j}} + \alpha^x x + \beta^x \left(\frac{1}{12} - x^2\right) + \alpha^y y + \beta^y \left(\frac{1}{12} - y^2\right) \tag{6}$$

where $\overline{\Phi_{i,j}}$ denotes the cell average within $V_{i,j}$, and both x and y are assumed to be in the range of $[-0.5, 0.5]$. Other coefficients are:

$$\alpha^x = \Phi^R_{i,j} - \Phi^L_{i,j}, \beta^x = 6\overline{\Phi_{i,j}} - 3(\Phi^R_{i,j} + \Phi^L_{i,j})$$
$$\alpha^y = \Phi^U_{i,j} - \Phi^D_{i,j}, \beta^y = 6\overline{\Phi_{i,j}} - 3(\Phi^U_{i,j} + \Phi^D_{i,j}) \tag{7}$$

$\Phi^L_{i,j}, \Phi^R_{i,j}, \Phi^U_{i,j}, \Phi^D_{i,j}$ represent the material distribution at each of the four boundary midpoints of a two-dimensional control volume and are obtained by cubical interpolation [CW84]. Figure 5 compares the visualization results between a piecewise constant and a quasi-parabolic material distribution function using the same vector field as in figure 1.

5. Implementation

The physically-based formulation for advection described in section 4 can be easily translated to implementation. Pseudocode can be found in the supplementary material at EG Digital Library [EGD08]. Details are provided in the following.

The two dimensional spatial domain is evenly discretized by $M \times N$ rectangular cells, each representing a control volume, $V^n_{i,j}$. The boundary edges of $V^n_{i,j}$ are defined by its corner points, which are shared with neighboring cells to avoid uncovered spatial regions caused by numerical inconsistency. Please refer to figure 6 (a). Each cell maintains the total mass of the dye material and the parameters in equation 7 derived from its neighboring cells. To achieve control volume based material transport, we first trace all corner points back in time using the standard Runge-Kutta 4th order numerical integration scheme. Each $V^{n-1}_{i,j}$, constructed with its corner points traced back in time (figure 6 (b)), is then used to perform intersection tests against the rectangular cells of the spatial domain to generate a set of intersection regions (figure 6(c)). In figure 6(d), the density distribution function Φ is integrated over the intersection region using Riemann sum. In all of our experiments 400 sample points are evenly distributed in each intersection cell. The density distribution function is evaluated on those that fall within the intersection region. To accelerate the intersection and integration process, we only consider rectangular cells overlapped with the bounding box of $V^{n-1}_{i,j}$ that contain non-zero mass.

dataset	Split	JP8	Karman
size (x,y,t)	64x64x10	200x200x400	768x231x1500
CV res	128x128	400x400	1536x462
time(sec)	532.8	10069.1	43213.2
mass change(%)	+3.2	-4.7	-5.1

Table 1: *Dataset statistics and timing numbers.*

6. Results and Discussion

We have implemented the proposed physically-based control volume transport scheme for two-dimensional dye advection in C++ on a standard Windows PC with 2.4 GHz Intel Core 2 Duo processor and 3 GB of system memory. The Computational Geometry Algorithms Library (CGAL) [CGA08] is utilized for polygon intersection. The statistics and performance numbers are reported in table 1.

Three flow datasets are used in experiments with the proposed physically based dye advection scheme. The visualization of dye advection is overlaid upon dense texture visualization showing instantaneous flow structures generated by GPUFLIC [LTH06]. `Split` (figure 1) is a synthetic flow showing a separating behavior. Figure 7 shows the visualization of the `JP8` dataset, which is an unsteady pool fire simulation of burning jet engine fuel. The top, middle, and bottom row of figure 7 compare the snapshots of the time sequence generated with the proposed algorithm, the texture advection scheme [JEH02], and the level-set method [Wei04], respectively. Compared to the proposed scheme, the texture advection method fails to faithfully convey detailed patterns due to excessive diffusion and mass loss. In the level-set method the upper structures in the flow are missing since the fast propagation of dye material in the proximity of the plume is com-

© 2008 The Author(s)
Journal compilation © 2008 The Eurographics Association and Blackwell Publishing Ltd.

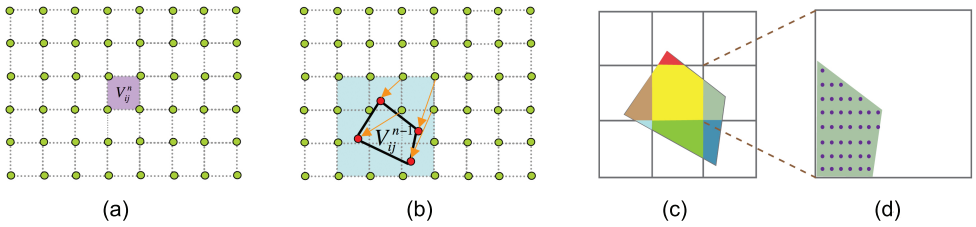

Figure 6: *Control volume advection and mass transport in 2D. (a) The spatial domain is discretized into control volumes sharing corner points. (b) Control volume V_{ij}^n advected back in time. Intersecting cells are shaded in light blue. (c) Intersection regions of $V_{i,j}^{n-1}$. (d) The local density distribution function is integrated over the intersection region using Riemann sum on sample points (purple).*

pletely suppressed by clamping. The third dataset used in our experiments is `Karman` (figure 8), a numerical simulation of the classical von Kármán vortex street phenomenon, where a repeating pattern of swirling vortices caused by the separation of flow passing over an obstacle. In this experiment, the patterns generated by the texture advection method are blurry due to numerical diffusion and loss of mass. In the level-set method, intricate structures are lost because of the binary dye/background threshold. Although the mass conservation is not perfectly achieved numerically due to inaccuracy caused by Riemann sum integration, this method is capable of conveying detailed structures not shown in the traditional texture-advection method thanks to physically based formulation. While the method is computationally expensive, we believe that interactivity can be achieved with a parallel implementation since equation 5 is intrinsically Lagrangian and our algorithm is therefore embarrassingly parallel.

7. Conclusion and Future Work

We have proposed a novel physically-based dye advection scheme for flow visualization. Unlike traditional texture advection based approaches, the proposed method is based on the concept of control volume analysis typically used in fluid dynamics. Due to its physically-based formulation, this method is capable of faithfully depicting detailed structural and temporal features in the underlying flow fields while avoiding any non-physical artifacts, which is not achievable with existing texture advection based methods. Combined with dense texture technique the proposed method can be used to accurately and effectively analyze the numerical datasets resulted from CFD simulations without loss of details. Although this method is computationally intensive, its control volume based formulation can easily lead to a parallel implementation for performance gains. In the future, we would like to pursue a GPU acceleration scheme of the proposed method for interactive visualization. Another possible avenue of future research is the extension to three-dimensional unstructured grids, which is the common practice in the CFD community to discretize the computational domain.

Acknowledgments

We would like to thank Daniel Weiskopf for providing leveset dye advection code. This work was made possible in part by United States NSF CNS-0551724, CCF-0541113, IIS-0513212; DOE ASC Alliance C-SAFE, SciDAC-VACET; and NIH/NCRR CIBC P41-RR12553-08.

References

[And95] ANDERSON J. D.: *Computational Fluid Dynamics*. McGraw-Hill, 1995.

[BFMF06] BRIDSON R., FEDKIW R., MULLER-FISCHER M.: Fluid simulation. SIGGRAPH 2006 course notes, 2006.

[BML95] BECKER B. G., MAX N. L., LANE D. A.: Unsteady flow volumes. In *VIS '95: Proceedings of the 6th conference on Visualization '95* (Washington, DC, USA, 1995), IEEE Computer Society, p. 329.

[BPL04] BOWLING L. C., POMEROY J. W., LETTENMAIER D. P.: Parameterization of blowing-snow sublimation in a macroscale hydrology model. *Journal of Hydrometeorology 5*, 5 (2004), 745–762.

[CC06] CENGEL Y., CIMBALA J.: *Fluid Mechanics: Fundamentals and Application*. McGraw-Hill Science/Engineering/Math, 2006.

[CGA08] CGAL, Computational Geometry Algorithms Library, 2008. http://www.cgal.org.

[CL93] CABRAL B., LEEDOM L. C.: Imaging vector fields using line integral convolution. In *SIGGRAPH '93: Proceedings of the 20th annual conference on Computer graphics and interactive techniques* (New York, NY, USA, 1993), ACM Press, pp. 263–270.

© 2008 The Author(s)
Journal compilation © 2008 The Eurographics Association and Blackwell Publishing Ltd.

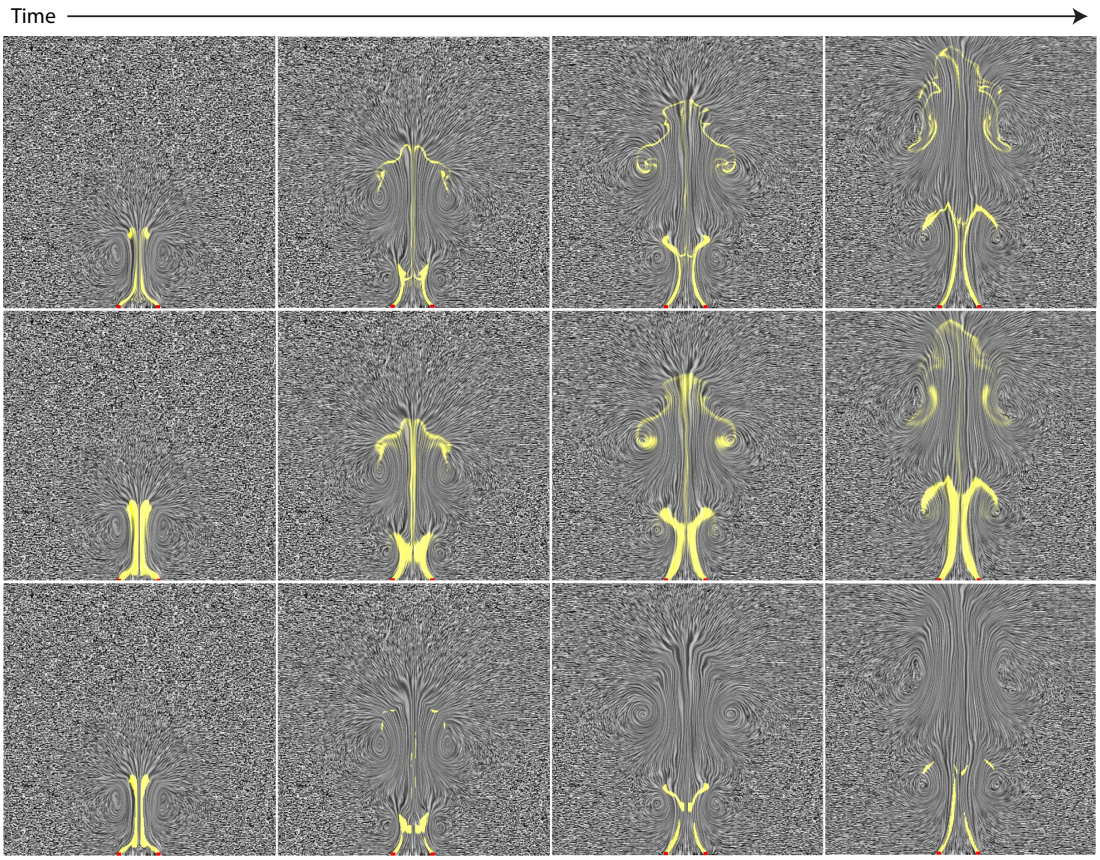

Figure 7: *Visualization of the JP8 dataset using dye advection. Top row: physically-based dye advection. Middle row: texture advection method. Bottom row: level-set method. The time sequence is from left to right.*

[CW84] COLELLA P., WOODWARD P.: The piecewise parabolic method (PPM) for gas-dynamical simulations. *Journal of Computational Physics 54* (1984), 174–201.

[EGD08] Eurographics Digital Library, 2008. http://www.eg.org/EG/DL.

[ETK*07] ELCOTT S., TONG Y., KANSO E., SCHRÖDER P., DESBRUN M.: Stable, circulation-preserving, simplicial fluids. *ACM Transactions on Graphics (TOG) 26*, 1 (2007), 4.

[FSJ01] FEDKIW R., STAM J., JENSEN H. W.: Visual simulation of smoke. In *SIGGRAPH '01: Proceedings of the 28th annual conference on Computer graphics and interactive techniques* (New York, NY, USA, 2001), ACM, pp. 15–22.

[JEH00] JOBARD B., ERLEBACHER G., HUSSAINI M. Y.: Hardware-accelerated texture advection for unsteady flow visualization. In *VIS '00: Proceedings of the conference on Visualization 2000* (Los Alamitos, CA, USA, 2000), IEEE Computer Society, pp. 155–162.

[JEH01] JOBARD B., ERLEBACHER G., HUSSAINI M. Y.: Lagrangian-eulerian advection for unsteady flow visualization. In *VIS '01: Proceedings of the conference on Visualization 2001* (Washington, DC, USA, 2001), IEEE Computer Society, pp. 53–60.

[JEH02] JOBARD B., ERLEBACHER G., HUSSAINI M.: Lagrangian-Eulerian advection of noise and dye textures for unsteady flow visualization. *IEEE Transactions on Visualization and Computer Graphics 8*, 3 (2002), 211–222.

[KK03] KARNIADAKIS G. M., KIRBY R. M.: *Parallel Scientific Computing in C++ and MPI*. Cambridge University Press, New York, NY, USA, 2003.

[KLLR07] KIM B., LIU Y., LLAMAS I., ROSSIGNAC J.: Advections with significantly reduced dissipation and diffusion. *IEEE Transactions on Visualization and Computer Graphics 13*, 1 (2007), 135–144.

[Lau06] LAURITZEN P.: An inherently mass-conservative semi-implicit semi-lagrangian model. Ph.d thesis: Department of Geophysics, University of Copenhagen, 2006.

[LP95] LAPRISE J. R., PLANTE A.: A class of semi-

© 2008 The Author(s)
Journal compilation © 2008 The Eurographics Association and Blackwell Publishing Ltd.

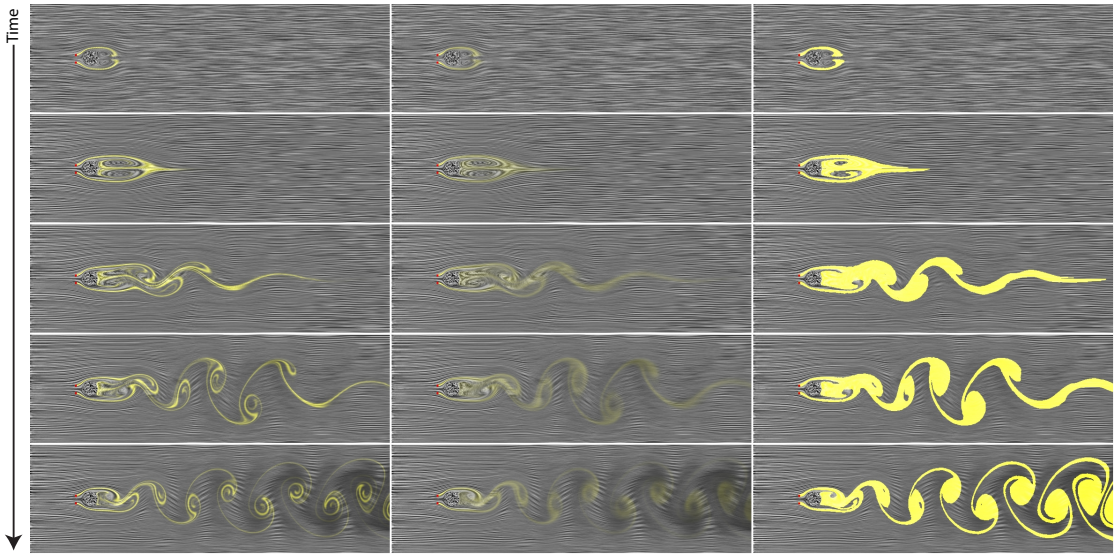

Figure 8: *Visualization of the Karman dataset using dye advection. Left column: physically-based dye advection. Middle column: texture advection method. Right column: level-set method. The time sequence is from top to bottom.*

lagrangian integrated-mass (slim) numerical transport algorithms. *Monthly Weather Review 123*, 2 (1995), 553–565.

[LTH06] LI G.-S., TRICOCHE X., HANSEN C.: GPU-FLIC: Interactive and accurate dense visualization of unsteady flows. In *Eurographics/IEEE-VGTC Symposium on Visualizations* (2006), pp. 29–34.

[MBC93] MAX N., BECKER B., CRAWFIS R.: Flow volumes for interactive vector field visualization. In *VIS '93 (1993): Proceedings of the 6th conference on Visualization '93* (1993), IEEE Computer Science Press, pp. 19–24.

[Mer87] MERZKIRCH W.: *Flow Visualization Second Edition*. Academic Press Inc. (London), 1987.

[NM02] NAIR R. D., MACHENHAUER B.: The mass-conservative cell-integrated semi-lagrangian advection scheme on the sphere. *Monthly Weather Review 130*, 3 (2002), 649–667.

[Rnc92] RNCIC M.: Semi-lagrangian piecewise biparabolic scheme for two-dimensional horizontal advection of a passive scalar. *Monthly Weather Review 120*, 7 (1992), 1394–1406.

[SJM96] SHEN H.-W., JOHNSON C., MA K.-L.: Visualizing vector fields using line integral convolution and dye advection. In *VIS '96: Proceedings of the 6th conference on Visualization '96 (San Francisco, CA, USA)* (1996), IEEE Computer Society Press, pp. 63–70.

[SKFS05] SCHMEJA S., KLESSEN R. S., FROEBRICH D., SMITH M. D.: Star formation from gravoturbulent fragmentation:. mass accretion and evolution of protostars. *Memorie della Societa Astronomica Italiana 76* (2005), 193–210.

[SP92] SMOLARKIEWICZ P. K., PUDYKIEWICZ J. A.: A class of semi-Lagrangian approximations for fluids. *Journal of Atmospheric Sciences 49* (Nov. 1992), 2082–2096.

[SS04] SUN W.-Y., SUN M.-T.: Mass correction applied to semi-lagrangian advection scheme. *Monthly Weather Review 132*, 4 (2004), 975–984.

[Sta99] STAM J.: Stable fluids. In *SIGGRAPH '99: Proceedings of the 26th annual conference on Computer graphics and interactive techniques* (New York, NY, USA, 1999), ACM Press/Addison-Wesley Publishing Co., pp. 121–128.

[SWK03] STANISLAS M., WESTERWEEL J., KOMPENHANS J.: *Particle Image Velocimetry: Recent Improvements: Proceedings of the EUROPIV 2 Workshop*. Springer, 2003.

[vW02] VAN WIJK J. J.: Image based flow visualization. In *ACM Transactions on Graphics (TOG)* (New York, NY, USA, 2002), ACM Press, pp. 745–754.

[WBE05] WEISKOPF D., BOTCHEN R. P., ERTL T.: Interactive visualization of divergence in unsteady flow by level-set dye advection. In *SimVis* (2005), pp. 221–232.

[Wei04] WEISKOPF D.: Dye advection without the blur: A level-set approach for texture-based visualization of unsteady flow. *Computer Graphics Forum 23*, 3 (2004), 479–488.

© 2008 The Author(s)
Journal compilation © 2008 The Eurographics Association and Blackwell Publishing Ltd.